ELSEVIER

Journal of Alloys and Compounds 234 (1996) 93–100

Journal of ALLOYS AND COMPOUNDS

Hydriding properties of the intermetallic compounds $Zr(Mn_{1-y}Nb_y)_x$ ($x = 0.97$–2.91, $y = 0$–0.208)

T. Kodama, H. Kaminaka

Research and Development Center, Sumitomo Metal Industries Ltd., 1-8 Fusocho, Amagasaki, Hyogo 660, Japan

Received 12 December 1994; revised 8 June 1995

Abstract

Pressure-composition (P–C) isotherm and X-ray diffraction measurements on $Zr(Mn_{1-y}Nb_y)_x$ ($x = 0.97$–2.91, $y = 0$–0.208; 26 charges) have been carried out. The equilibrium pressure decreases and the lattice parameter increases with increasing Nb addition. The hydrogen capacity of non-stoichiometric $Zr(Mn_{1-y}Nb_y)_x$ (hypo-Zr) is nearly proportional to the total number of Zr2Mn2, ZrNbMn2, Zr2MnNb and ZrMn2Nb interstices. Both $|\Delta H_A|$ and $|\Delta H_D|$ increase with increasing lattice parameter, with the former showing a clearer dependence than the latter. ΔS_A shows a weak dependence on the lattice parameter, but ΔS_D shows no dependence at all. Both $\Delta H_A/\Delta S_A$ and $\Delta H_D/\Delta S_D$ display a strong dependence on the lattice parameters. The degree of slope of the plateau in the P–C isotherm is nearly proportional to $|\Delta H|\Delta_c(2\theta)$, where $\Delta_c(2\theta)$ is the corrected halfwidth of the X-ray diffraction profile.

Keywords: Intermetallic compounds; Hydrogen storage; Hydriding properties

1. Introduction

The intermetallic compound $ZrMn_x$ is a hydrogen storage material which is characterized by rapid reaction with hydrogen at comparatively high temperature. The hydriding properties of this compound change with x [1–6] and the effects of adding third and fourth elements have been studied by many investigators and reviewed by Ivey and Northwood [7].

The addition of niobium to $ZrMn_x$ lowers the hydrogen equilibrium pressure [8]. In this work other hydriding properties of $Zr(Mn_{1-y}Nb_y)_x$($x = 0.97$–2.91, $y = 0$–0.208) have been studied. The changes in the hydrogen capacity, the thermodynamic parameters and the degree of slope of the plateau pressure in the pressure–composition (P–C) isotherm with x and y have been determined.

The relationship between the hydrogen capacity of the non-stoichiometric compound and the number of specific tetrahedral interstices has been discussed. The preferred sites for H atoms have been assumed to be the Zr2Mn2 interstice and the tetrahedral interstices in which only an Nb atom is substituted for a Zr or Mn atom composing the Zr2Mn2 interstice on the basis of neutron diffraction measurements by Didisheim et al. [9] on $ZrMn_2D_3$ and Pontonnier et al. [10] on $ZrMn_xD_{3.10-3.26}$ ($x = 2$, 2.5, 2.75). The numbers of these interstices have been calculated based on the site occupancies of Mn atoms in non-stoichiometric $ZrMn_x$ [2,10–12] and Nb atoms in $Zr(Mn_{1-y}Nb_y)_x$ [12].

The changes in the thermodynamic parameters (enthalpy change and entropy change) with x and y obtained by van't Hoff plots have been discussed in relation to the lattice parameter.

Luo et al. [4] have explained that the slope of the plateau in the P–C isotherm for $ZrMn_x$ is caused by an increase in the enthalpy change with H content. They [5] have also proposed that a spread of certain thermodynamic parameters leads to sloping plateaux and that this spread may arise from segregation of the constituent elements. Yonezu et al. [13] have explained that a compound with sharp X-ray profiles shows a smaller slope than one with broad X-ray profiles. A modification of these propositions has been proposed in order to explain the slopes obtained in this work.

0925-8388/96/$15.00 © 1996 Elsevier Science S.A. All rights reserved
SSDI 0925-8388(95)01935-9

2. Experimental methods

Button ingots of about 0.15 kg mass were double melted by arc melting in an argon atmosphere. The raw materials used were reactor grade zirconium sponge, electrolytic manganese and electrolytic niobium. The ingots were analysed by inductively coupled plasma mass spectrometry. The chemical compositions were as follows:

(1) binary compounds $ZrMn_x$
$x = 0.98$–2.91; 11 charges
(2) ternary compounds $Zr(Mn_{1-y}Nb_y)_x$
$x = 0.97$, 1.20, $y = 0.05(0.050, 0.053)$; two charges
$x = 0.98$–2.89, $y = 0.11(0.100$–$0.109)$; eight charges
$x = 0.98$–2.90, $y = 0.21(0.204$–$0.210)$; five charges.

Both the absorption and desorption P–C isotherms were measured. Coarse granules were inserted in a pressure vessel, activated by evacuation and hydrogenation (about 5 MPa) twice at room temperature and evacuated at 973 K for 1 h in order to ensure complete dehydrogenation before the start of measurements. The main measurement temperatures were 473 and 573 K. Some specimens were also measured at 290, 373 K and other temperatures.

X-Ray diffraction (XRD) measurements were carried out in order to obtain the lattice parameters and the broadening of the XRD profiles. The radius r_s derived from the volume per atom, known as the Seitz radius [14,15], was used as a comparative measure of the lattice parameters. The Seitz radius was calculated from the lattice parameter as follows:

$$\frac{4}{3}\pi r_s^3 = \frac{\text{volume of unit cell}}{\text{number of atoms in cell}}$$

The broadening of the XRD profiles for the $ZrMn_2$ phase was measured as the halfwidth ($\Delta(2\theta)$ at half-maximum) of the diffraction profiles from the (110), (103), (112) and (201) planes, which showed comparatively stronger intensities. The four values were arithmetically averaged. Details of the X-ray diffraction measurements have been given in Ref. [12].

The above measurements were carried out on as-cast specimens. However, some specimens were also measured under heat-treated conditions in order to study the effects of heat treatment. The heat treatment conditions were as follows:

(1) annealing condition
1073 K for 5 h in vacuum: $ZrMn_x$($x = 0.98$, 1.26, 1.33, 1.95, 2.42)
1273 K for 5 h in vacuum: $ZrMn_x$($x = 2.02$)
(2) oil-quenching (OQ) condition
1273 K for 5 h, then OQ in vacuum: $ZrMn_x$ ($x = 0.98$, 1.33).

3. Results and discussion

3.1. P–C isotherms

The P–C isotherms for the as-cast compounds $Zr(Mn_{1-y}Nb_y)_{1.0}$, $Zr(Mn_{1-y}Nb_y)_{2.2}$ and $Zr(Mn_{1-y}Nb_y)_{2.9}$ are shown in Fig. 1 as examples of the P–C isotherms obtained in this work. According to van Essen and Buschow [1], those for as-cast $ZrMn_x$ show complex features (two-stage plateau or no plateau) while those for annealed specimens show simple features (a single plateau). However, our as-cast specimens show simple features. Little differences between as-cast and annealed specimens has been observed.

The P–C isotherms for $Zr(Mn_{1-y}Nb_y)_{1.0}$ are shifted along the x axis. This shift is caused by α-Zr and/or Zr-rich phases which coexist with the $ZrMn_2$ phase [6,8]. In some cases residual hydrogen is observed as has been reported by Nishimiya [3].

3.2. Hydrogen capacities of non-stoichiometric $Zr(Mn_{1-y}Nb_y)_x$ (hypo-Zr)

The hydrogen capacities of non-stoichiometric $ZrMn_x$ ($x = 2.21$, 2.91) decrease with increasing x as shown in Fig. 1. Those of non-stoichiometric $Zr(Mn_{1-y}Nb_y)_x$ seem to increase with increasing y. It is expected that the hydrogen capacity is proportional to the number of preferred sites for H atoms. Thus the relationship between the hydrogen capacity and the number of specific tetrahedral interstices has been studied.

According to neutron diffraction experiments by Didisheim et al. on $ZrMn_2D_3$ [9] and Pontonnier et al. on $ZrMn_xD_n$ ($x = 2$, 2.5, 2.75) [10], the occupancy site for D atoms is the Zr2Mn2 interstice. The number of Zr2Mn2 interstices in non-stoichiometric $ZrMn_x$ (hypo-Zr) can be easily calculated, because the occupancy site for stoichiometrically excess Mn atoms is the A site [2,10–12]. The partition of the constituent atoms into their occupancy sites and the number of Zr2Mn2 interstices per atom [16] are expressed as follows:

$ZrMn_x = (Zr_{1-z}Mn_a)Mn_2 = AB_2$
$a = (x - 2)/(x + 1)$
number of Zr2Mn2 interstices per atom $= 4(1 - a)^2$

When the hydrogen capacity of the ternary compound $Zr(Mn_{1-y}Nb_y)_x$ is related to the number of

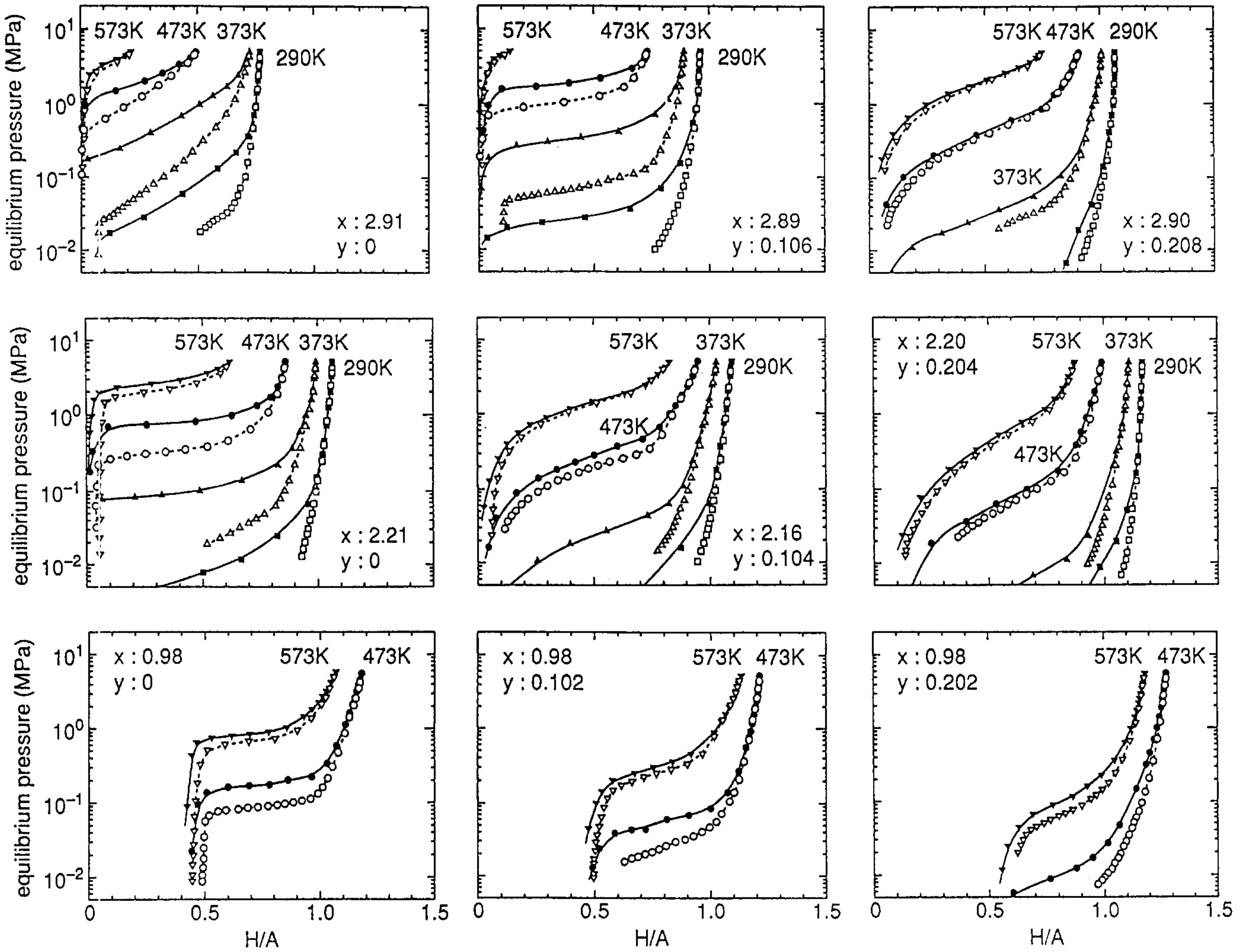

Fig. 1. P–C isotherms for as-cast $Zr(Mn_{1-y}Nb_y)_{1.0}$, $Zr(Mn_{1-y}Nb_y)_{2.2}$ and $Zr(Mn_{1-y}Nb_y)_{2.9}$. Full symbols represent absorption and open symbols desorption.

preferred sites for H atoms, it is necessary that the preferred sites be assumed, because they have not been obtained experimentally. The preferred sites have been assumed to be the Zr2Mn2 interstice and the interstices in which only an Nb atom is substituted for a Zr or Mn atom composing the Zr2Mn2 interstice. The numbers of these interstices can be calculated based on the site occupancies of Nb atoms [12]. Nb atoms in non-stoichiometric $Zr(Mn_{1-y}Nb_y)_x$ (hypo-Zr) are first substituted for Mn atoms in the A sites and then occupy the B sites after Mn atoms in the A sites are exhausted. Thus the partitions of the constituent atoms are expressed as follows:

$$
\begin{aligned}
Zr(Mn_{1-y}Nb_y)_x &\rightarrow (Zr_{1-a-b}Mn_aNb_b)(Mn_{1-c}Nb_c)_2 \\
x &> 2 \\
&\rightarrow (Zr_{1-a-b}Mn_aNb_b)Mn_2 \\
y &\leqslant (x-2)/3x \\
a &= (-3xy + x - 2)/(x+1) \\
b &= 3xy/(x+1) \\
&\rightarrow (Zr_{1-b}Nb_b)(Mn_{1-c}Nb_c)_2 \\
y &\geqslant (x-2)/3x \\
b &= (x-2)/(x+1) \\
c &= (3xy - x + 2)/2(x+1)
\end{aligned}
$$

The numbers of specific interstices derived from the original A2B2 and AB3 interstices are given in Table 1.

The relationships between the hydrogen capacity (H/A) and the total number of Zr2Mn2, ZrNbMn2, Zr2MnNb and ZrMn2Nb interstices (N_T/A) are shown in Fig. 2. The hydrogen capacity was determined as H/A which showed a pressure of 5 MPa on the P–C isotherm. It seems that the hydrogen capacity is approximately proportional to the total number of specific interstices, although slight differences are seen among $y = 0$ ($ZrMn_x$), 0.11 and 0.21. The proportionality relationships between H/A and N_T/A shown

Table 1
Numbers of interstices

Interstice[a]		Number of specific interstices per atom	
Original	Derived	$y \leqslant (x-2)/3x$	$y \geqslant (x-2)/3x$
A2B2	$\text{Zr2}\underline{\text{Mn2}}$	$4(1-a-b)^2$	$4(1-b)^2(1-c)^2$
	$\text{ZrNb}\underline{\text{Mn2}}$	$8(1-a-b)b$	$8(1-b)b(1-c)^2$
	$\text{Zr2}\underline{\text{MnNb}}$	0	$8(1-b)^2(1-c)c$
AB3	$\text{Zr}\underline{\text{Mn2Nb}}$	0	$4(1-b)(1-c)^2c$

[a] The underlining indicates the B site atoms in the stoichiometric compound AB_2.

in Fig. 2 have been obtained under the condition that the proportionality coefficient is common to $y = 0$, 0.11 and 0.21 for simplicity. If the binding energies between H atoms and interstices are different among the specific interstices, then the relationships between the temperature and the hydrogen occupancy ratio of the interstices differ among the interstices according to the Maxwell–Boltzmann distribution [17]. However, it has been assumed in Fig. 2 that the occupancy ratio is the same among the four interstices.

The changes in the hydrogen capacity and the numbers of specific interstices with x are shown in Fig. 3, where the numbers of specific interstices have been adjusted at each temperature by the common proportionality coefficient between H/A and N_T/A. The hydrogen capacities of $ZrMn_x$ at 290 and 373 K deviate at larger x from the number of Zr2Mn2 interstices. These deviations are probably caused by sites which cannot be preferred sites in the stoichiometric compound becoming occupied as the distances of neighbouring H atoms increase. The H/A values determined in this work agree well with those in the literature, except for two references which have reported H/A at 323 K [1,5]. Those for $y = 0.11$ agree with the numbers excluding the ZrMn2Nb interstice which is derived from the AB3 interstice. Those for $y = 0.21$ agree with the numbers including the $\text{Zr}\underline{\text{Mn2Nb}}$ interstice. Although the reason for the difference between $y = 0.11$ and 0.21 is uncertain, one possible explanation might be as follows.

The lattice parameters and lattice strains for the compounds with $y = 0.21$ are larger than those for the compounds with $y = 0.11$ [12]. Thus it is estimated that the radius of the $\text{Zr}\underline{\text{Mn2Nb}}$ interstice in the compounds with $y = 0.21$ is larger than in the compounds with $y = 0.11$ and that the $\text{Zr}\underline{\text{Mn2Nb}}$ interstice in the compounds with $y = 0.21$ can be easily occupied by H atoms, although the radius of the AB3 interstice is slightly smaller than that of the A2B2 interstice in the stoichiometric compound AB_2 [16].

In any case it is almost certain that the preferred sites for H atoms in non-stoichiometric $Zr(Mn_{1-y}Nb_y)_x$ are at least the $\text{Zr2}\underline{\text{Mn2}}$, $\text{ZrNb}\underline{\text{Mn2}}$ and $\text{Zr2}\underline{\text{MnNb}}$ interstices which are derived from the A2B2 interstice. The possibility that the $\text{Zr}\underline{\text{Mn2Nb}}$ interstice which is derived from the AB3 interstice also contributes a preferred site cannot be denied. The hydrogen capacity is approximately proportional to the total number of these interstices.

3.3. Thermodynamic parameters

The enthalpy changes ΔH_A and ΔH_D and entropy changes ΔS_A and ΔS_D ($\Delta S = 0$ at 0.1 MPa) have been obtained using van't Hoff plots (subscripts A and D denote absorption and desorption respectively). The equilibrium pressures at $\Theta = \frac{1}{2}$(Θ is the fraction of H/A with respect to the maximum H/A for the $ZrMn_2$ phase) were used in calculating the parameters, since

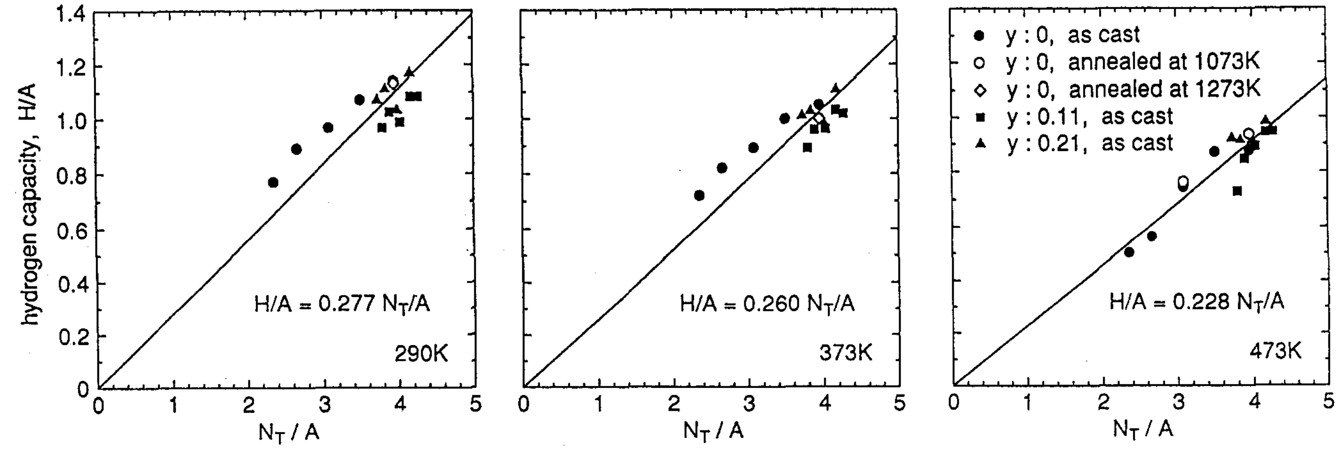

Fig. 2. Relationships between hydrogen capacity and total number of specific tetrahedral interstices for $Zr(Mn_{1-y}Nb_y)_x$ ($x = 2.02$–2.91, $y = 0$–0.210). N_T is the total number of the Zr2Mn2, ZrNbMn2, Zr2MnNb and ZrMn2Nb interstices.

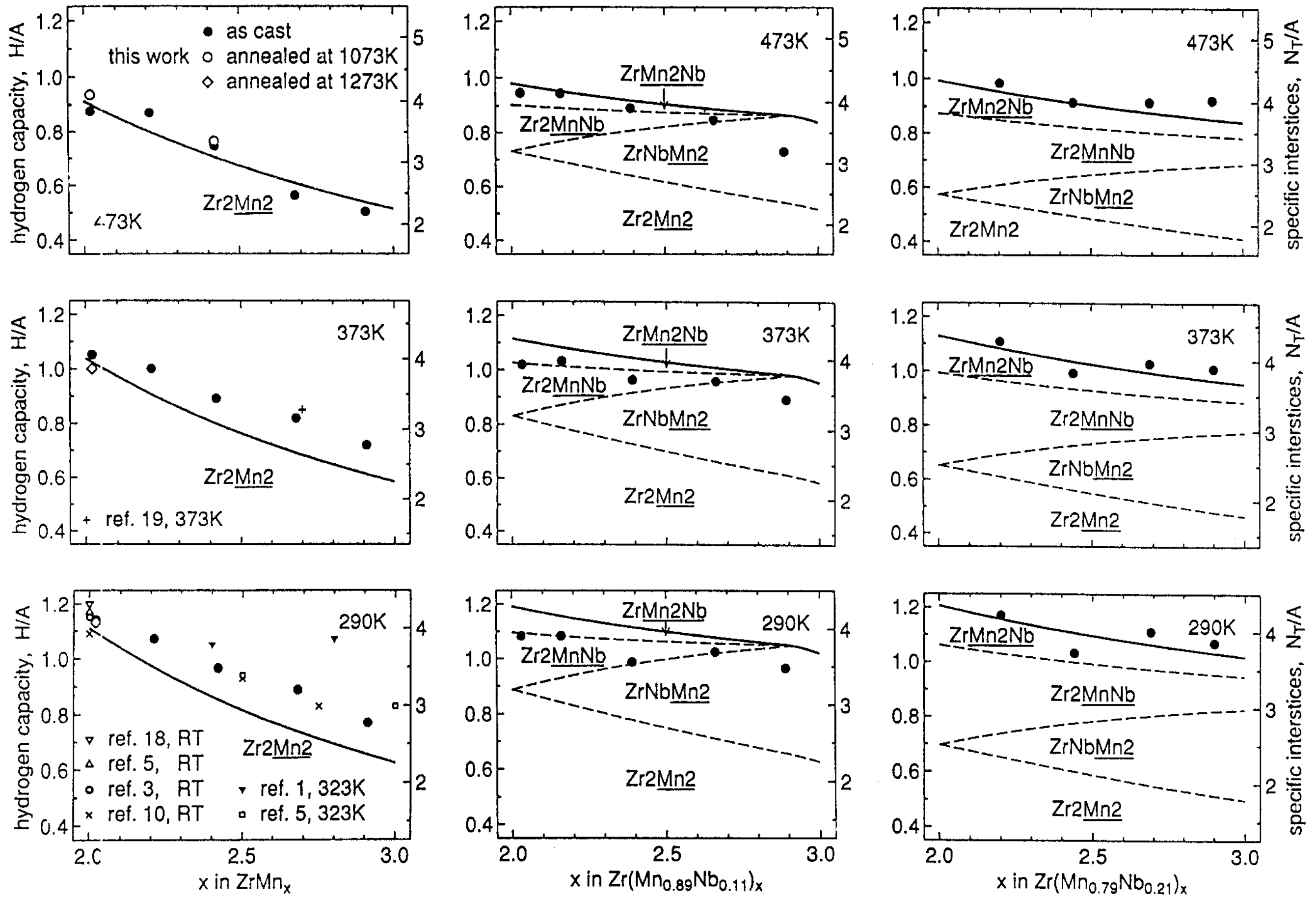

Fig. 3. Changes in hydrogen capacity and numbers of specific tetrahedral interstices with x for $ZrMn_x$, $Zr(Mn_{0.89}Nb_{0.11})_x$ and $Zr(Mn_{0.79}Nb_{0.21})_x$. Full circles represent the hydrogen capacity (H/A) and lines the numbers of specific interstices (N/A). The underlining indicates the B site atoms in the stoichiometric compound AB_2.

the effect of Θ on the parameters was small, as has been reported by Pourarian et al. [2]. The effect of Θ on the parameters for $Zr(Mn_{0.790}Nb_{0.210})_{2.44}$, which showed the largest slopes in this work, is presented as an example in Table 2.

The parameters ΔH and ΔS for $ZrMn_x$ are shown in Fig. 4. There is little difference between as-cast and heat-treated samples. $|\Delta H_D|$ and $|\Delta S_D|$ are larger than $|\Delta H_A|$ and $|\Delta S_A|$ respectively. Calorimetrically determined $|\Delta H_A|$ and $|\Delta H_D|$ values in the literature [2,5,6,20] generally range between $|\Delta H_A|$ and $|\Delta H_D|$ found in this work. Both the enthalpy change and entropy change determined from van't Hoff plots by Uchida et al. [19] agree well with this work.

The relationships between the Seitz radius and these parameters are shown in Fig. 5. ΔH_A displays a clear dependence on the lattice size. This dependence is the same as that obtained by Ogawa and Ohnishi [21] for $LaNi_{5-x}A_x$ (A ≡ Al, Cr, V, Fe, Cu). The dependence of ΔH_D on the lattice size is not as clear as that of ΔH_A. ΔS_A shows a weak dependence on the Seitz radius, but ΔS_D shows no dependence at all. The relationships between the Seitz radius and the parameter $\Delta H/\Delta S$ are also shown in Fig. 5. Very strong correlations which

Table 2
Effect of Θ on thermodynamic parameters

Θ	H/A	ΔH_A (kJ $molH_2^{-1}$)	ΔH_D (kJ $molH_2^{-1}$)	ΔS_A (J K^{-1} $molH_2^{-1}$)	ΔS_D (J K^{-1} $molH_2^{-1}$)
$\frac{1}{4}$	0.54	−45.3	−49.5	−84.5	−91.8
$\frac{1}{2}$	0.27	−42.6	−47.4	−91.0	−99.0

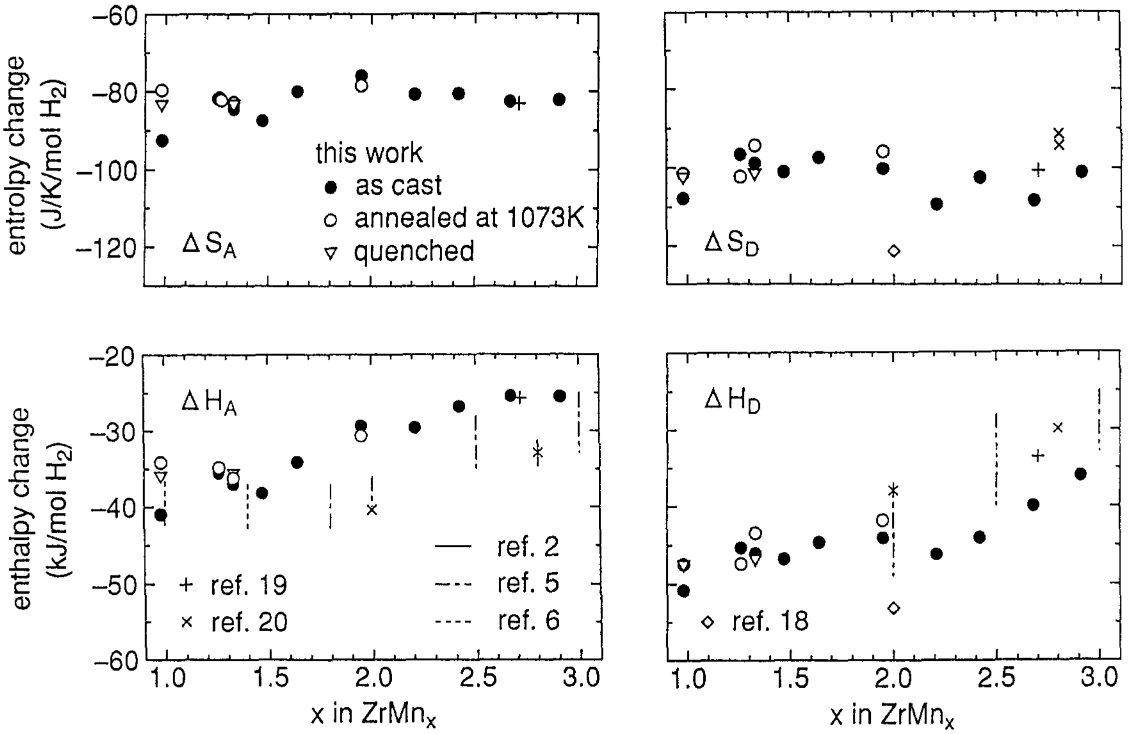

Fig. 4. Enthalpy change and entropy change for $ZrMn_x$.

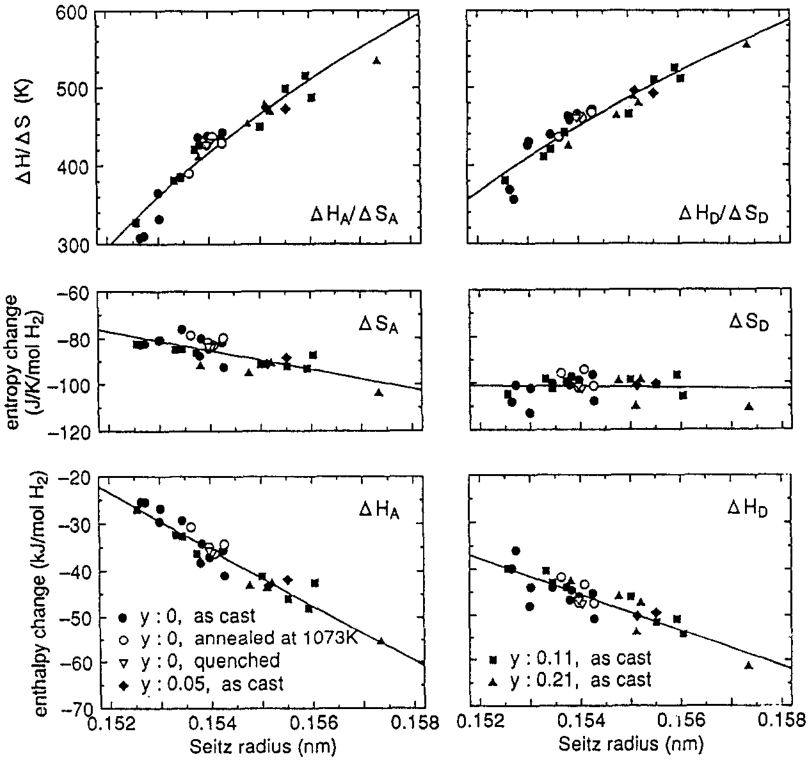

Fig. 5. Effects of Seitz radius on enthalpy change, entropy change and $\Delta H/\Delta S$.

seem to indicate parabolic relations are recognized in both absorption and desorption, although the physical and/or chemical meanings are not clear. This parameter indicates the temperature corresponding to the equilibrium pressure of 0.1 MPa on the pressure–temperature (P–T) diagram and can be called the characteristic temperature for a hydrogen-absorbing material.

The regression expressions for the above parameters are given in Table 3.

3.4. Slopes of plateaux

The degree of slope was determined as $\Delta(\ln P)/\Delta\Theta$ by averaging at several temperatures. The degrees of slope of the plateaux show complex variations among specimens. The slopes for $ZrMn_x$ are shown in Fig. 6. Our results for $ZrMn_x$ show nearly the same tendencies as those of Luo et al. [4,5], who have reported that the degree of slope for $ZrMn_x$ increases with the degree of non-stoichiometry. Those for $Zr(Mn_{1-y}Nb_y)_{2.9}$ decrease at first and then increase with y as shown in Fig. 1. The variation in the degree of slope appears to depend on the halfwidth $\Delta(2\theta)$ of the XRD profile [12]. The degree of slope during desorption is usually larger than that during absorption for the hypo-Zr compound.

Luo et al. [4] have explained that the slope is caused by an increase in the enthalpy change with H content. They [5] have also proposed that a spread of certain thermodynamic parameters leads to sloping plateaux and that this spread may arise from segregation of the constituent elements. Yonezu et al. [13] have explained that the reason why $ZrMn_{1.6}Co_{0.2}V_{0.2}$ shows a smaller slope than $ZrMn_{1.8}V_{0.2}$ is that the former displays sharper X-ray profiles than the latter.

Table 3
Regression expressions for thermodynamic parameters (r_s in nanometers)

Regression expression	Correlation coefficient
ΔH_A (kJ $molH_2^{-1}$) = $893.6 - 6033r_s$	0.95
ΔH_D (kJ $molH_2^{-1}$) = $556.2 - 3907r_s$	0.87
ΔS_a (J K^{-1} $molH_2^{-1}$) = $554.8 - 4156r_s$	0.76
ΔS_D (J K^{-1} $molH_2^{-1}$) = $-60.0 - 271r_s$	0.07
$\Delta H_A/\Delta S_A$ (K) = $6583(r_s - 0.1500)^{1/2}$	0.96
$\Delta H_D/\Delta S_D$ (K) = $5852(r_s - 0.1481)^{1/2}$	0.94

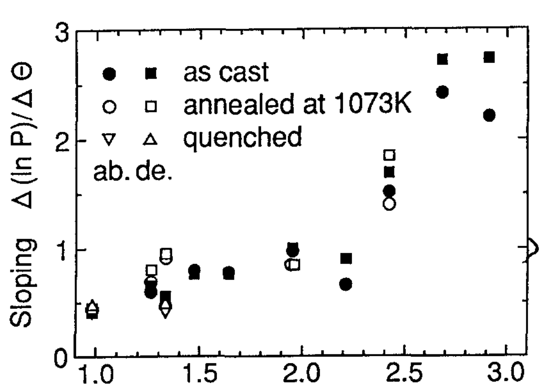

Fig. 6. Slopes in P–C isotherms for $ZrMn_x$.

We have modified the discussions by Luo et al. and Yonezu et al. It is easily reasoned that the processes described below proceed during absorption and desorption in the compound with a spread of the enthalpy change. During absorption, H atoms begin to occupy the sites with stronger $|\Delta H_A|$ at the beginning of the plateau, then occupy the sites with medium $|\Delta H_A|$ and finally occupy the sites with weaker $|\Delta H_A|$ at the end of the plateau. During desorption, H atoms begin to leave the sites with weaker $|\Delta H_D|$ at the beginning and finally leave the sites with stronger $|\Delta H_D|$ at the end. Thus the equilibrium pressure in the plateau region increases with increasing H content and a slope arises. The cause of this slope is the spread of the enthalpy change. It is estimated that this spread is approximately proportional to $|\Delta H|\Delta_c(2\theta)$, where $\Delta_c(2\theta) = [\Delta^2(2\theta) - \Delta^2_{min}(2\theta)]^{1/2}$, $\Delta(2\Theta)$ is the halfwidth of the XRD profile and $\Delta_{min}(2\theta)$ is the minimum halfwidth in this work (0.208°).

The relationships between the degree of slope $\Delta(\ln P)/\Delta\Theta$ and the spread parameter $|\Delta H|\Delta_c(2\theta)$ are shown in Fig. 8, including both absorption and desorption. Considerable agreement is seen between them. The regression expressions between them are given in Table 4.

The variations in the halfwidths in this work do not arise from segregation of the component elements but from strain induced by the site occupancies of the component atoms. Thus it can be concluded that the degree of slope is strongly influenced by the spread of the enthalpy change through the spread of the size of the preferred sites for H atoms. The slopes for the

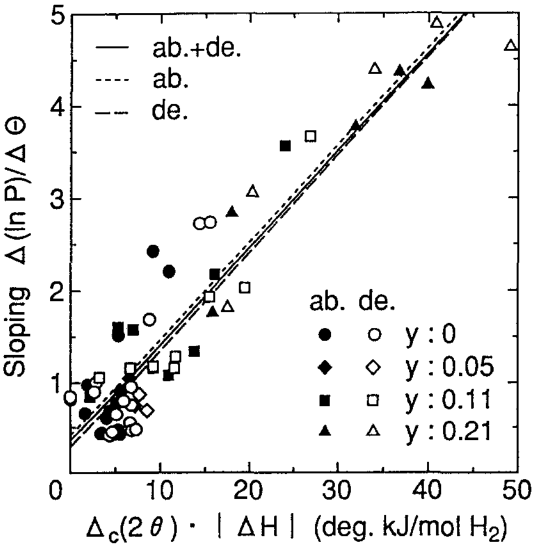

Fig. 7. Relationships between slopes in P–C isotherms and parameter $|\Delta H|\ \Delta_c(2\theta)$.

Table 4
Regression expressions between degree of slope and spread parameter

Regression expression	Correlation coefficient
$\Delta(\ln P_A)/\Delta\Theta = 0.41 + 0.106\,\lvert\Delta H_A\rvert\Delta_c(2\theta)$	0.93
$\Delta(\ln P_D)/\Delta\Theta = 0.28 + 0.106\,\lvert\Delta H_D\rvert\Delta_c(2\theta)$	0.94
$\Delta(\ln P)/\Delta\Theta = 0.35 + 0.105\,\lvert\Delta H\rvert\Delta_c(2\theta)$[a]	0.93

[a] Both absorption and desorption are included.

quaternary compounds $Zr(Mn_{1-y-z}Nb_yFe_z)_{1.35}$ ($y = 0$–0.2, $z = 0$–0.2) have also shown a clear dependence on $\lvert\Delta H\rvert\Delta_c(2\theta)$ [22].

4. Conclusions

(1) P–C isotherm and X-ray diffraction measurements on $Zr(Mn_{1-y}Nb_y)_x$ ($x = 0.97$–2.91, $y = 0$–0.208) have been carried out.

(2) The equilibrium pressure decreases and the lattice parameter increases with increasing Nb addition.

(3) The hydrogen capacity of non-stoichiometric $Zr(Mn_{1-y}Nb_y)_x$ (hypo-Zr) is nearly proportional to the total number of Zr2Mn2, ZrNbMn2, Zr2MnNb and ZrMn2Nb interstices. The first three are derived from the A2B2 interstice and the last one from the AB3 interstice.

(4) Both $\lvert\Delta H_A\rvert$ and $\lvert\Delta H_D\rvert$ increase with increasing lattice parameter. The former shows a clearer dependence than the latter. ΔS_A shows a weak dependence on the lattice parameter, but ΔS_D shows no dependence at all. Both $\Delta H_A/\Delta S_A$ and $\Delta H_D/\Delta S_D$ display a strong dependence on the lattice parameter.

(5) The degree of slope of the plateau in the P–C isotherm is nearly proportional to $\lvert\Delta H\rvert\Delta_c(2\theta)$, where $\Delta_c(2\theta)$ is the corrected halfwidth of X-ray diffraction profile.

References

[1] R.M. van Essen and K.H.J. Buschow, *Mater. Res. Bull.*, *15* (1980) 1149.

[2] F. Pourarian, V.K. Sinha, W.E. Wallace, A.T. Pedziwiatr and R.S. Craig, in P. Jena and C.B. Satterthwaite (eds.), *Proc. Int. Symp. on Electronic Structure and Properties of Hydrogen in Metals, Richmond, VA, 1982*, Plenum, New York, 1983, p. 385.

[3] N. Nishimiya, *Mater. Res. Bull.*, *21* (1986) 1025.

[4] W. Luo, S. Majorowski, J.D. Clewley and T.B. Flanagan, *Z. Phys. Chem. NM.F.*, *163* (1989) 81.

[5] W. Luo, J.D. Clewley, T.B. Flanagan and W.A. Oates, *J. Alloys Comp.*, *185* (1992) 321.

[6] T.B. Flanagan, H. Noh, W. Luo and W.A. Oates, *J. Alloys Comp.*, *185* (1992) 339.

[7] D.G. Ivey and D.O. Northwood, *Z. Phys. Chem. N.F.*, *147* (1986) 191.

[8] T. Kodama, H. Anada and Y. Yoshinaga, *Proc. MRS Int. Meet. on Advanced Materials*, Vol. 2, Materials Research Society, Pittsburgh, PA, 1989, p. 57.

[9] J.J. Didisheim, K. Yvon and D. Shaltiel, *Solid State Commun.*, *31* (1979) 47.

[10] L. Pontonnier, S. Miraglia, D. Fruchart, J.L. Soubeyroux, A. Baudry and P. Boyer, *J. Alloys Comp.*, *186* (1992) 241.

[11] F. Pourarian, H. Fujii, W.E. Wallace, V.K. Sinha and H.K. Smith, *J. Phys. Chem.*, *85* (1981) 3105.

[12] T. Kodama, H. Anada and H. Kaminaka, *J. Alloys Comp.*, *224* (1995) 70.

[13] I. Yonezu, S. Fujitani, A. Furukawa, K. Nasako, T. Yonesaki, T. Saito and N. Furukawa, *J. Less-Common Met.*, *168* (1991) 201.

[14] H.J. King, *J. Mater. Sci.*, *1* (1966) 79.

[15] C.S. Barrett and T.B. Massalski, *Structure of Metals*, McGraw-Hill, New York, 3rd edn., 1966.

[16] C.B. Magee, J. Liu and C.E. Lundin, *J. Less-Common Met.*, *78* (1981) 119.

[17] Y.-B. Wang and D.O. Northwood, *Mater. Sci. Technol.*, *4* (1988) 97.

[18] D. Shaltiel, I. Jacob and D. Davidov, *J. Less-Common Met.*, *53* (1977) 117.

[19] M. Uchida, H. Bjurstrom, S. Suda and Y. Matsubara, *J. Less-Common Met.*, *119* (1986) 63.

[20] A.T. Pedziwiatr, R.S. Craig, W.E. Wallace and F. Pourarian, *J. Solid-State Chem.*, *46* (1983) 336.

[21] T. Ogawa and K. Ohnishi, *J. Jpn. Soc. Heat Treat.*, *29* (1989) 254.

[22] T. Kodama and H. Kaminaka, in preparation.